Materials Research. 2019; 22(suppl. 2): e20180921
DOI: http://dx.doi.org/10.1590/1980-5373-MR-2018-0921

Investigation on Electrical Properties and Microdefects of Nb^{5+}-Doped $BaTiO_3$ Based Ceramics by Positron Annihilation Techniques

***Xuxin Cheng*[a]*, *Yuxin Wang*[b], *Xiaoming Chen*[a], *Haining Cui*[a]**

[a]*School of Electronic and Electrical Engineering, Zhaoqing University, Zhaoqing Road, Duanzhou District, Zhaoqing 526061, Guangdong, PR China*
[b]*School of Materials Science and Engineering, Jiangsu University of Science and Technology, Zhenjiang 212003, Jiangsu, China*

Received: December 23, 2018; Revised: April 02, 2019; Accepted: April 30, 2019

The influence of the Nb^{5+}-doped content and the doping $CaCO_3$ on the electrical properties and the microdefects of BSTN ceramics by Positron Annihilation Techniques were studied, which were fired at 1350 °C for 2 hours in air. The PTCR characteristics in the BSTN samples were also investigated. Moreover, the information on microdefects in BSTN ceramics was demonstrated by coincidence Doppler broadening spectrum measurements and positron annihilation lifetime spectra. Meanwhile, the influence of the defects on the electrical properties of the ceramics was also revealed. Furthermore, the critical donor-dopant content was 0.4 mol%, which corresponding room-temperature resistivity and the resistivity jumping ratio was 714.3 Ω·cm and 2.77×10^2, respectively. In addition, the average positrons annihilate lifetime τ of the BSTN ceramics was investigated as well.

Keywords: *$BaTiO_3$, PTC effect, Positron annihilation, Defect, Electroceramics.*

1. Introduction

Barium titanate is a ferroelectric material, which transforms from a tetragonal perovskite structure (ABO_3) into a paraelectric structure [1]. The ions at the A or B site of $BaTiO_3$ are replaced by small quantities of a trivalent donor or pentavalent impurities, respectively; $BaTiO_3$ becomes a semiconducting material and exhibits the positive temperature coefficient of resistivity (PTCR) effect [2, 3]. Heywang [4] explained this phenomenon, and an improved discussion was later provided by Jonker [5].The PTCR characteristic of doped $BaTiO_3$ ceramics is considered to a grain-boundary effect.

An effective method is considered to detect defects in bulk by positron annihilation technology (PAT) [6, 7], which include the coincidence Doppler broadening spectrum (CDBS) and positron annihilation lifetime spectra (PALS). The momentum distribution of the annihilating e^+–e′ pairs can be detected using the CDBS; meanwhile, the annihilation information of positrons can be offered by the PALS. Recently, Deng et al. [8] suggested that the Nb addition was effective in enhancing the d–d interactions by Positron Annihilation Techniques (PAT). The defects of the $ZnNb_{2-x}Ti_xO_{6-x}$ ceramics could be also investigated by PAT [9]. The PALS of TiAl alloys had been analyzed [10]. In addition, a high amount of titanium vacancies could lead to grain-growth inhibition [11]. The precipitation of a Ti-rich phase was due to a vacancy-compensation mechanism [12]. Thus, the charge compensation was achieved by titanium vacancies and electrons [13].

However, little attention has been paid to the donor-doped content on both the electrical properties and the microdefects of the BSTN ceramics. Previous studies have focused only on the chemical reaction of the samples. Therefore, the objective of this study is to investigate the effects of the donor-doped content and the doping $CaCO_3$ on the microdefects and the electrical properties of BSTN ceramics using the PAT.

2. Experimental Procedures

The starting materials were high-purity $BaCO_3$ (>99.8%), $SrCO_3$ (>99.8%), Nb_2O_5 (>99.99%), TiO_2 (>99.8%), Al_2O_3 (>99.8%), and SiO_2 (>99.99%), and they were weighed on the basis of the following formula: $(Ba_{0.95}Sr_{0.05})(TiNb_x)O_3$ + $Mn(NO_3)_2$ + 0.25 mol% ($4Al_2O_3$: $9SiO_2$: $3TiO_2$) (BSTN), In our work, the samples doped with 0.2, 0.3, 0.4 and 0.5 mol% Nb^{5+} were represented as SP1, SP2, SP3 and SP4; Moreover, the SP3 ceramics of doping $CaCO_3$ with 4 mol% and 8 mol% were replaced by SP5 and SP6, respectively. The mixture was mixed by wet ball milling for 8 h in deionized water using an agate ball in a polyurethane jar, and they were dried at 115 °C in drying oven, then the powders were calcined at 1190 ºC for 3 h in air. The mixture was ground again through ball-milling for 8 h. The dried powders were mixed with PVA and compacted by pressing at 150MPa to prepare the green compacts (φ15mm × 3mm size). The blocks were sintered in an aluminum tube at 1350 ºC for 2 h in air.

* e-mail: cxx101@126.com

Moreover, the surfaces of the fired BSTN ceramics were coated Ag-Zn alloy and then sintered at 540 °C for 10 min in order to form electrodes, thereafter the room-temperature (RT) resistance of the specimens was measured using a digital multimeter, and the temperature dependence of resistance was measured in a temperature-programmable furnace at a heating rate of 1.6 ºC/min in the range of 25–300 ºC. In addition, the surface microstructure of the sintered ceramics was observed using scanning electron microscopy (SEM; S-3400N Hitachi, Japan). The average grain size of the ceramics was estimated by the line-intersection method.

The PALS were carried out at room temperature using a fast–fast coincidence ORTEC system with a time resolution of 240 ps (full width at half maximum, FWHM). A 3.7×10^5 Bq source of ^{22}Na was sandwiched between two sheets of the samples [10].

The CDBS were measured by sandwiching a 0.6 MBq ^{22}Na radioactive source, supported by two kapton films, between two pieces of the same sample. The CDBS were carried out by a two-detector coincidence system. A high purity Ge (HPGe) detector with a resolution of 1.3 keV at 511 KeV was determined to be the main detector. A NaI(Tl) scintillator was decided to the auxiliary detector supplying the coincidence signal, which was located in collinear geometry with the Ge detector for detecting the two 511 keV γ rays from the e^+–e^- annihilation pair. A peak with about 10^7 counts to background ratio of approximate 1.5×10^4 on the high-energy side of the peak could be obtained in the peak of each spectrum. The CDBS of signal crystals of Si, and BSTN ceramics have been measured.

3. Results and Discussion

3.1. Microstructure of the ceramics

The microstructure of the BSTN ceramics with doping $CaCO_3$ of different contents sintered at 1350 °C for 2 h in air is shown in Fig. 1. A slight difference in the grain size is observed. The average grain sizes of the samples doped Ca^{2+} of 0–8 mol% are 6.88 μm, 4.47 μm, and 2.80 μm, respectively. It indicates that the grain size of the specimens decreases quickly with an increase of the concentration of $CaCO_3$; Moreover, the grain size of the SP6 samples becomes very uniform in Fig.1 (c), probably due to the inhibition of the grain growth with an increase in the $CaCO_3$ content. Thus, the particle-size distribution may be due to differences in the rates of grain growth.

3.2. XRD analysis

The XRD patterns of the BSTN ceramics prepared by firing at 1350 °C for 2 h are shown in Fig. 2. The diffraction peaks of the samples exhibit a tetragonal structure in which the reflections (002) and (200) can be split into two peaks at room temperature. Moreover, the peak position where (111) is shifted to higher 2θ with the increase of Ca^{2+} may be due to the smaller interplanar distance, as calculated by the Bragg equation.

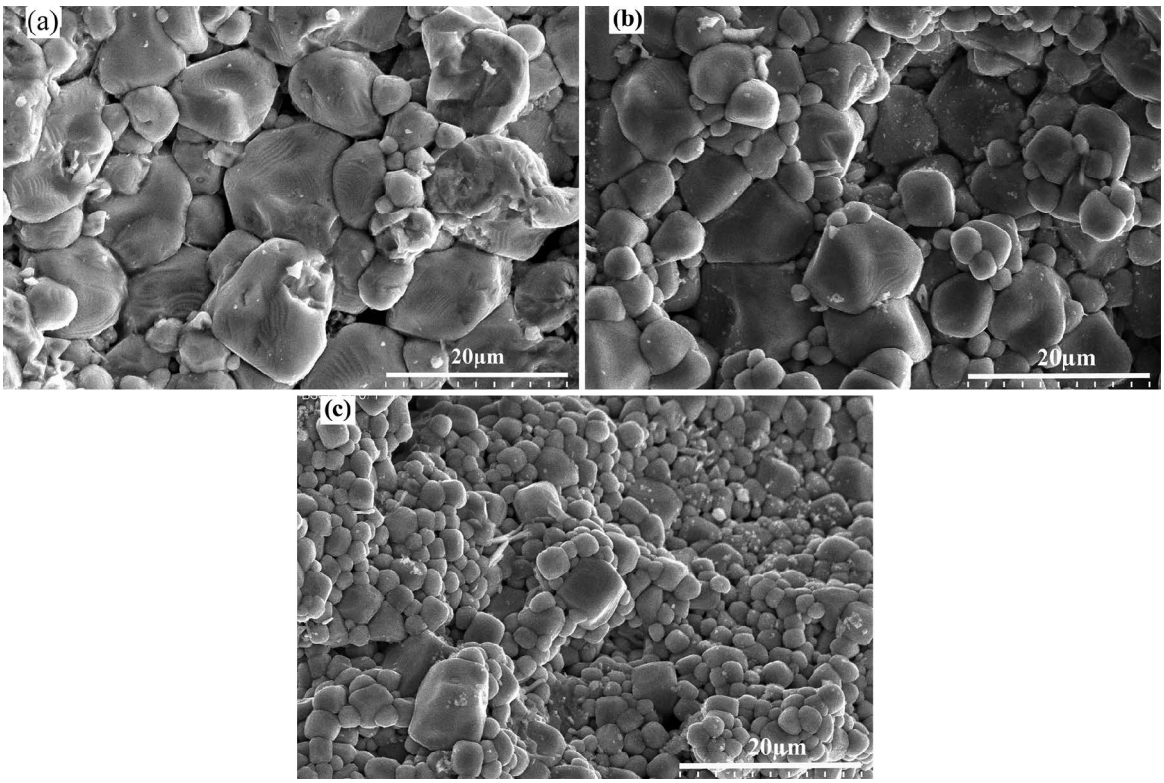

Figure 1. The SEM micrograph on the surfaces of the BSTN ceramics doped $CaCO_3$ with different content; (a) 0 mol%, (b) 4 mol%, (c) 8 mol%.

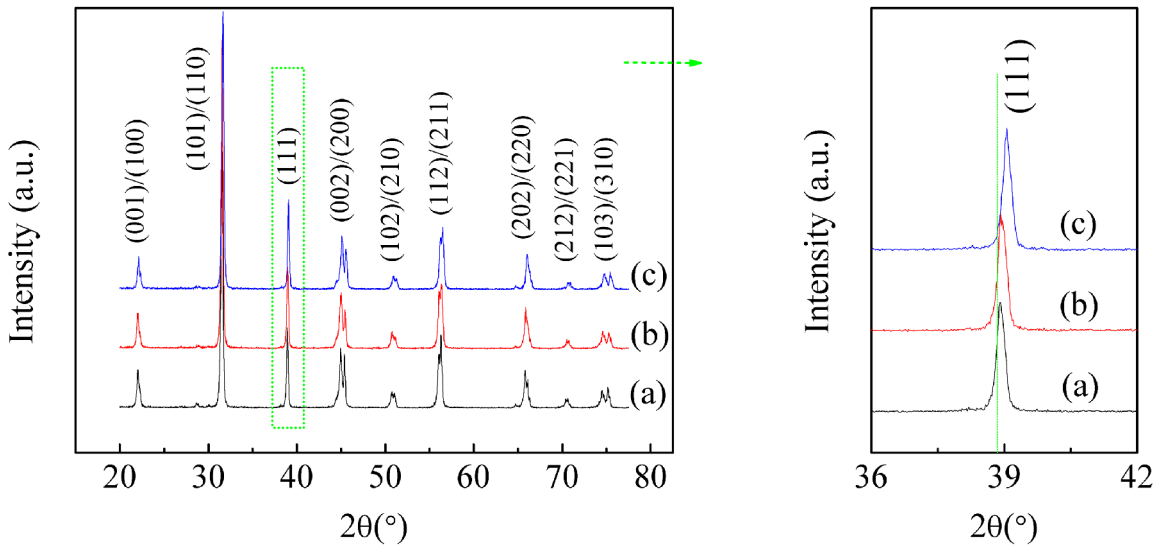

Figure 2. XRD patterns of BSTN ceramics doped $CaCO_3$ with various content; (a) 0 mol%, (b) 4 mol%, (c) 8 mol%.

3.3. Electrical properties and the resistivity jumping ratio of the BSTN ceramics

The dependence of the RT resistivity and the resistivity jumping ratio (ρ_{max}/ρ_{min}) of the BSTN ceramics on the dopant content is shown in Table 1. From the table, the RT resistivity can be found to decrease firstly and then increase with an increase in the content of doping Nb^{5+} of 0.2−0.5 mol%; however, the trend of the resistivity jumping ratio as a function of the dopant concentration is contrary to that of the RT resistivity. The results show that the critical donor-dopant content is 0.4 mol% Nb^{5+}. The corresponding RT resistivity and the resistivity jumping ratio is 714.3 Ω·cm and 2.77×10^2. The phenomenon signifies that the decrease in resistivity is due to the electron compensation of the substitution of Ti^{4+} by Nb^{5+} [13, 14]. However, the increase in resistivity is generally attributed to the ionic compensation resulting from the formation of cation vacancies [15-17]. In addition, we can see that the higher the doping Ca^{2+} content, the higher is the RT resistivity as well. This is because the doping $CaCO_3$ may be beneficial to the grain refinement in BSTN ceramics. But the resistivity jumping ratios of the SP5 and SP6 samples are far lower than that of the SP3. Furthermore, the temperature coefficient of resistance (α_T) of the BSTN samples is nearly affected by the dopant content in Table 1.

3.4. Parameters of PALS of the BSTN ceramics

The defects in the BSTN samples can be characterized by the PALS. The spectra of the ceramics are analyzed by three decay lifetime (τ_1,τ_2 and τ_3) and the corresponding intensities (I_1', I_2' and I_3') [18] after background subtractions and source corrections. The τ_3 in each sample has long decay lifetime (> 1844 ps) and a small intensity I_3' (< 1%). This is because that the positrons are annihilated at the surface of samples, so it can be not considered in our experiment. Thus, the total intensities of I_1' and I_2' must be re-normalized and be labeled as I_1 and I_2, respectively. The τ_2 is the annihilated lifetime of the positron at the defect, its corresponding annihilated rate $\lambda_d = \tau_2^{-1}$. On the base of the standard two-state trapping model [19], the positron annihilated rate λ_b and lifetime τ_b in the bulk are calculated for the following formula, $\lambda_b = I_1\tau_1^{-1} + I_2\tau_2^{-1}$ and $\tau_b = \lambda_b^{-1}$, respectively. While the average lifetime τ is based on the following equation, $\tau = I_1\tau_1 + I_2\tau_2$. Finally, the electron densities in defects and bulk, n_d and n_b, can be be expressed as the following formula [20]: $n = (\tau\text{-}2) / 134$, respectively. The characteristic parameters of the positron annihilate lifetime of the BSTN ceramics are shown in Table 2. Moreover, Fig. 3 shows that the dependent of the τ and n_b of the ceramics in Table 2 on the Nb^{5+}-doped content.

Table 1. The electrical properties and the resistivity jumping ratio of the BSTN samples

Sample	Nb^{5+}/ mol%	$CaCO_3$/mol%	ρ_{25}/Ω·cm	α_T/%·ºC^{-1}	ρ_{max}/ρ_{min}
SP1	0.2	0	1754.4	3.1	131.8
SP2	0.3	0	911.1	3.1	130.9
SP3	0.4	0	714.3	4.8	276.7
SP4	0.5	0	1815.6	3.4	128.6
SP5	0.4	4	14263.8	4.1	27.0
SP6	0.4	8	18232.7	4.5	47.2

Table 2. The parameters of the positron annihilation lifetime spectra of the BTSN ceramics.

Sample	τ_1 / ps	τ_2 / ps	I_1 / %	I_2 / %	λ_b / ns^{-1}	λ_d / ns^{-1}	n_b / ×10-2a.u.	n_d / ×10^{-2}a.u.	τ / ps
SP1	193±3	393±34	92.5	7.5	4.98	2.54	2.23	0.41	208.00
SP2	192±2	429±48	93.9	6.1	5.03	2.33	2.26	0.25	206.46
SP3	193±2	402±47	92.5	7.5	4.98	2.49	2.22	0.36	208.68
SP4	199±3	478±67	94.7	5.3	4.87	2.09	2.14	0.07	213.79

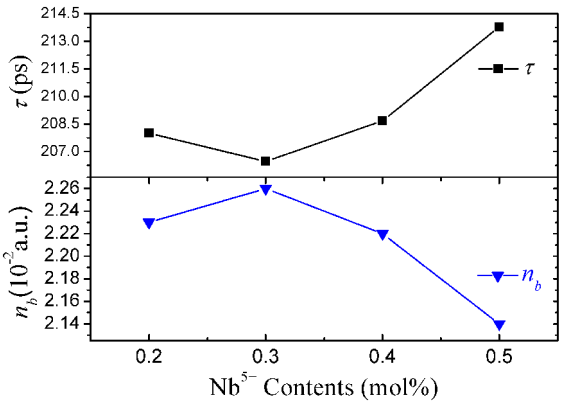

Figure 3. The average lifetime τ of the positrons and the free electron density n_b in the BSTN samples is as a function of the Nb_2O_5 content.

The mean positron annihilate lifetime τ increases firstly and then decreases with the increasing of the donor-doped concentration; however, the change trend of the electron densities in bulk n_b is just contrary to that of the τ in Fig. 3. Furthermore, it is found that the τ (206.46 ps) of the SP2 samples is minimum, this is because that the n_b (2.26×10^{-2} a.u.) in the SP2 bulk is maximum at the same time. In addition, the electronic configuration of Nb and Ti are $4d^4\ 5s^1$ and $3d^2\ 4s^2$, respectively. The d electron of Nb is more than that of Ti. Moreover, the electronic energy level of Nb (4d) is also higher than that of the Ti (3d). The conductivity characteristics are considered by electron compensation when the Ti in the BSTN ceramics (0.2 mol% < x < 0.3 mol%) is substituted by Nb. The results have been proved by the experimental data of the τ. But an increase in the τ is attributed to the vacancies compensation mechanism.

3.5. CDBS analysis of the BSTN samples

The background of the Doppler broadening spectrum can be reduced by the coincidence technique. In view of the constituent of the longitudinal horizontal momentum P_L of the annihilation e^+–e^- pair the 511 keV site is broadened into (511 + ΔE) keV site. Moreover, the P_L is given by the expression: $P_L = 2\ \Delta E / c$, where ΔE is the frequency shift, and c is the velocity of light. In order to convenient for identifying various spectral lines, the ratio curves can be obtained by the comparison of every spectral line and the standard spectrum of Si.

The ratio curves for the SP1−SP6 samples with doping different dopant which are sintered at 1350 °C in air is shown as in Fig. 4. The constituent of the longitudinal momentum P_L of the annihilation e^+–e^- pair in 10^{-3} m_0c is regarded as X-axis. The detailed shape of the high-momentum part of the Doppler spectrum is determined by the different effects from the positron annihilation with the electrons of each shell of the atom.

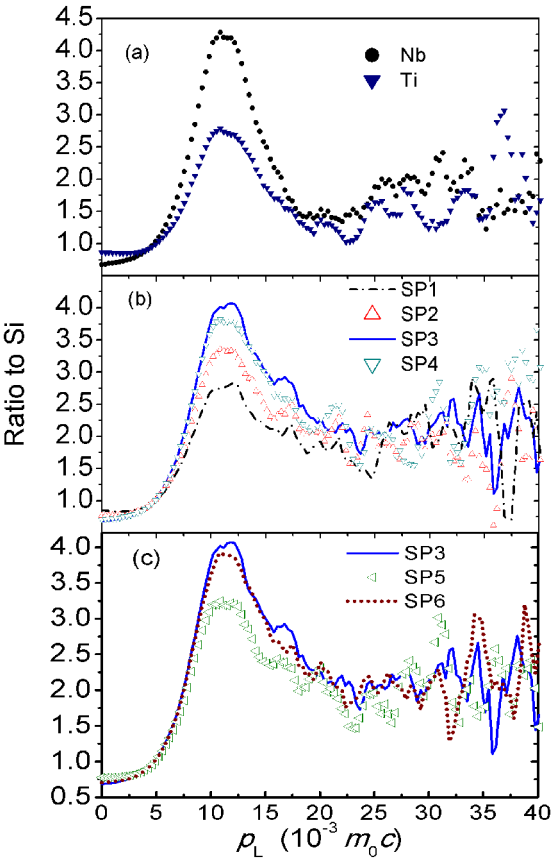

Figure 4. The ratio curves for the samples; (a) Nb and Ti ratio curves; (b) The SP1, SP2, SP3 and SP4 ratio curves, (c) The SP3, SP5 and SP6 ratio curves; The reference sample is Si.

It is showed that the main peak of the ratio curves of the BSTN samples cooled at 1100 °C for 2 h after firing at 1350 °C for 2 h in air increases at first and then decreases with the increasing of the donor-doped content in the Fig. 4.

The Nb and Ti ratio curves show a peak at about 10.85×10^{-3} m_0c in Fig. 3(a); the intensities of the pecks are 4.28 and 2.79, respectively. These peaks are due to the positron annihilation with d electrons [8, 21]. Furthermore, the peaks of each BSTN samples lie between 2.79−4.28. The increase in the peak is because that the Ti is substituted by Nb. It is indicated that the annihilation of the e^+-e^- pair is related to the donor-doped concentration. The intensities of the peck near 11.84×10^{-3} m_0c for the SP3 specimens are more than that of the other samples; Moreover, the intensities of the maximum peak of the ceramics is 4.07. The formation of the peck at about 11.84×10^{-3} m_0c is generally attributed to the annihilation of positrons and 2p electrons of oxygen atoms. It is inferred that the difference of the peak position of the samples with doping the same dopant is due to the annihilation of positron and 3d electrons of the cations, which can be obtained by the formation of the defect in the BSTN ceramics. Especially, lots of the titanium vacancies in the BSTN samples can be formed. Moreover, the bigger the content of the cation vacancies, the higher is the peak of the annihilation of positron with 3d electrons.

4. Conclusions

The influence of the Nb^{5+}-doped content and the $CaCO_3$ on the electrical properties and the microdeffect of the BSTN ceramics were investigated by PALS and DSMB Techniques, which were fired at 1350 °C for 2 h in air. The results indicated that the donor-doped content affected the formation of the microdefects and the electrical properties of the BSTN specimens. Moreover, both the RT resistivity and the positron annihibition lifetime τ of the BSTN ceramics decreased firstly and then increased with the increasing of the Nb^{5+}-doped content. The critical donor-doped content is 0.4 mol%, which corresponding average positrons annihilate lifetime τ is 208.68 ps. meanwhile, It is found that the major peak of the ratio curves of the SP3 sample is lie in about 11.84×10^{-3} m_0c.

5. Acknowledgements

This work was financially supported by the National Natural Science Foundation of China (No. 51402258), the Natural Science Foundation of Guangdong Province (No. 2015A030313706), the Science and Technology Planning Project of Guangdong Province (No. 2014A010105056), the Characteristic Creative Project in University of Guangdong Province (No. 2016KTSCX152), the Science and Technology Planning Project of Zhaoqing City (No. 201804030402).

6. References

1. Mancini MW, Paulin Filho PI. Direct observation of potential barriers in semiconducting barium titanate by electric force microscopy. *Journal of Applied Physics*. 2006;100(10):104501.

2. Illingsworth J, Al-Allak HM, Brinkman AW, Woods J. The influence of Mn on the grain-boundary potential barrier characteristics of donor-doped $BaTiO_3$ ceramics. *Journal of Applied Physics*. 1990;67(4):2088-2092.

3. Heywang W. Resistivity Anomaly in Doped Barium Titanate. *Journal of the American Ceramic Society*. 1964;47(10):484-490.

4. Heywang W. Bariumtitanat als sperrschichthalbleiter. *Solid-State Electronics*. 1961;3(1):51-58.

5. Jonker GH. Some aspects of semiconducting barium titanate. *Solid-State Electronics*. 1964;7(12):895-903.

6. Pikart P, Hugenschmidt C, Horisberger M, Matsukawa Y, Hatakeyama M, Toyama T, et al. Positron annihilation in Cr, Cu, and Au layers embedded in Al and quantum confinement of positrons in Au clusters. *Physical Review B*. 2011;84(1):014106.

7. Wang D, Chen ZQ, Wang DD, Qi N, Gong J, Cao CY, et al. Positron annihilation study of the interfacial defects in ZnO nanocrystals: Correlation with ferromagnetism. *Journal of Applied Physics*. 2010;107(2):023524.

8. Deng W, Guo JT, Brusa RS, Karwasz GP, Zecca A. Effects of Zr and Nb on d electrons in NiAl alloy studied by coincidence positron annihilation spectroscopy. *Materials Letters*. 2005;59(27):3389-3392.

9. Tang Y, Zhang Y, Du PY, Deng W. Direct Control of Defects on Positron Lifetimes and Dielectric Constant of Microwave Ceramics. *Journal of the American Ceramic Society*. 2013;96(8):2537-2543.

10. Deng W, Huang YY, Wu DH, Cao MZ, Xiong LY. Effects of Cr and Sn on defects and electron densities in TiAl alloys. *Materials Letters*. 2002;56(4):593-596.

11. Brzozowski E, Castro MS. Grain growth control in Nb-doped $BaTiO_3$. *Journal of Materials Processing Technology*. 2005;168(3):464-470.

12. Langhammer HT, Makovec D, Pu Y, Abicht HP, Drofenik M. Grain boundary reoxidation of donor-doped barium titanate ceramics. *Journal of the European Ceramic Society*. 2006;26(14):2899-2907.

13. Chan HM, Harmer MR, Smyth DML. Compensating Defects in Highly Donor-Doped $BaTiO_3$. Journal of the American Ceramic Society.1986;69(6):507-510.

14. Pu Y, Wu H, Wei J, Wang B. Influence of doping Nb^{5+} and Mn^{2+} on the PTCR effects of $Ba_{0.92}Ca_{0.05}(Bi_{0.5}Na_{0.5})_{0.33}TiO_3$ ceramics. *Journal of Materials Science: Materials in Electronics*. 2011;22(9):1479.

15. Brzozowski E, Castro MS, Foschini CR, Stojanovic B. Secondary phases in Nb-doped $BaTiO_3$ ceramics. *Ceramics International*. 2002;28(7):773-777.

16. Nowotny J, Rekas M. Defect structure, electrical properties and transport in Barium Titanate. VII. Chemical diffusion in Nb-doped $BaTiO_3$. Ceramics International. 1994;20(4):265-275.

17. Brzozowski E, Castro MS. Influence of Nb^{5+} and Sb^{3+} dopants on the defect profile, PTCR effect and GBBL characteristics of $BaTiO_3$ ceramics. *Journal of the European Ceramic Society*. 2004;24(8):2499-2507.

18. Kirkegaard P, Eldrup M. Positronfit extended: A new version of a program for analysing position lifetime spectra. *Computer Physics Communications*. 1994;7(7):401-409.

19. Brandt W, Paulin R. Positron Diffusion in Solids. *Physical Review B*. 1972;5(7):2430.

20. Brandt W, Reinheimer J. Theory of Semiconductor Response to Charged Particles. *Physical Review B*. 1970;2(8):3104.

21. Ghosh VJ, Alatalo M, Asoka-Kumar P, Nielsen B, Lynn KG, Kruseman AC, et al. Calculation of the Doppler broadening of the electron-positron annihilation radiation in defect-free bulk materials. *Physical Review B*. 2000;61(15):10092.